Current Research in Biotechnology 4 (2022) 211–220

Contents lists available at ScienceDirect

Current Research in Biotechnology

journal homepage: www.elsevier.com/locate/crbiot

Polyhydroxyalkanoates from industrial cheese whey: Production and characterization of polymers with differing hydroxyvalerate content

Mónica Carvalheira [a,b,*], Loic Hilliou [c], Catarina S.S. Oliveira [a,b,1], Eliana C. Guarda [a,b], Maria A.M. Reis [a,b]

[a] Associate Laboratory i4HB – Institute for Health and Bioeconomy, NOVA School of Science and Technology, NOVA University Lisbon, 2819-516 Caparica, Portugal
[b] UCIBIO – Applied Molecular Biosciences Unit, Department of Chemistry/Department of Life Sciences, NOVA School of Science and Technology, NOVA University Lisbon, 2819-516 Caparica, Portugal
[c] Institute for Polymers and Composites, University of Minho, Campus de Azurém, 4800-058 Guimarães, Portugal

ARTICLE INFO

Keywords:
Pilot Scale
Cheese whey valorization
Biodegradable biopolymers
Hydroxyvalerate content
Thermal properties

ABSTRACT

The composition of polyhydroxyalkanoate (PHA) monomers affects the properties and final applications of PHA polymers. This study focused on the feasibility of producing tailored PHA differing in hydroxyvalerate (HV) content, through manipulation of the acidogenic fermented stream composition, and on the characterization of PHA properties to determine the best composition for melt processing. Cheese whey was used as a feedstock, and changes in the organic loading rate during acidogenic fermentation led to the production of a fermented stream with an HV precursor content of 9–33 wt%. In the PHA production assays, a PHA content of 50 ± 11 wt%. (VSS basis) and yield of 0.76 ± 0.14 $gCOD_{PHA}.gCOD_{FP}^{-1}$ were obtained. Fermented stream supplementation with HV precursors during the PHA accumulation assays indicated the feasibility of producing tailored PHA with differing HV content without a need for the selection of new cultures. The thermal properties of PHA were found to be controlled by the HV content, and PHA with approximately 30 wt% HV had the lowest melting temperature. These results demonstrated the robustness of the process at pilot scale, thus supporting full-scale applications in tailored PHA production.

Introduction

Currently, increasing awareness of the use of environmentally friendly products has resulted in greater interest in renewable resources as alternatives to petrochemical products. For example, polyhydroxyalkanoate (PHA) products are biobased, biocompatible and biodegradable polymers with numerous potential applications (Medeiros Garcia Alcântara et al., 2020; Oliveira et al., 2017). PHAs are natural polyesters that are produced by several microorganisms as carbon and energy reserves, and have mechanical and thermal properties similar to those of conventional plastics (Oliveira et al., 2017; Sabapathy et al., 2020). However, the industrial production of PHA remains limited by production costs as much as five times higher than those for petroleum plastics (Sabapathy et al., 2020), thus limiting their packaging applications. Therefore, decreasing the costs of PHA production is crucial to allow these methods competitive alternatives to conventional plastic production. One option is based on mixed microbial cultures (MMC), which enable the use of open systems (without a requirement for sterile conditions) and inexpensive feedstocks. Life cycle assessment and financial analyses have indicated that PHA production using MMC and renewable resources is an economically and environmentally attractive option (Gurieff and Lant, 2007). The feasibility of producing PHA at pilot scale has been demonstrated by using several industrial wastes or by-products, such as fruit waste (Matos et al., 2021), the organic fraction of municipal solid waste and/or waste activated sludge (Moretto et al., 2020; Morgan-Sagastume et al., 2015; Valentino et al., 2020, 2019, 2018), and potato-starch factory wastewater (Morgan-Sagastume et al., 2020). Cheese whey (CW), a by-product in the dairy industry, is composed mainly of lactose and provides a potential source of nutrients (proteins) (Oliveira et al., 2018). Therefore, this feedstock is of potential interest for acidogenic fermentation and subsequent PHA production.

* Corresponding author at: Associate Laboratory i4HB – Institute for Health and Bioeconomy, NOVA School of Science and Technology, NOVA University Lisbon, 2819-516 Caparica, Portugal; UCIBIO – Applied Molecular Biosciences Unit, Department of Chemistry/Department of Life Sciences, NOVA School of Science and Technology, NOVA University Lisbon, 2819-516 Caparica, Portugal
E-mail address: mic16141@fct.unl.pt (M. Carvalheira).
[1] Present address: CBQF-Centro de Biotecnologia e Química Fina – Laboratório Associado, Escola Superior de Biotecnologia, Universidade Católica Portuguesa, Rua Diogo Botelho 1327, 4169-005 Porto, Portugal.

https://doi.org/10.1016/j.crbiot.2022.03.004
Received 12 November 2021; Revised 18 March 2022; Accepted 21 March 2022

Indeed, CW has been used to produce PHA at laboratory scale and to select MMC at pilot scale (Duque et al., 2014; Oliveira et al., 2018, 2017; Valentino et al., 2015).

Different types of PHA, most commonly polyhydroxybutyrate (PHB) and polyhydroxy(butyrate-co-valerate) (PHBV), are produced from wastes by MMC. The properties of PHA markedly vary depending on the monomeric composition and molecular weight.

The incorporation of HV monomers decreases brittleness, thus making the polymer more flexible and enhancing processability (Keskin et al., 2017). Moreover, PHBV has better thermal properties, notably a lower melting temperature, than PHB. Consequently, the thermal degradation of the polymer is limited, thus overcoming challenges in converting PHA into packaging products through conventional processing technologies (Cunha et al., 2016; Hilliou et al., 2016a).

PHA monomers with differing composition can be obtained by supplying the microbial population with different precursors. In the MMC process, the first step, acidogenic fermentation, involves fermentation of the feedstock to produce precursors for PHA, which are obtained through the conversion of organic matter into volatile fatty acids (VFAs). The second step, culture selection, consists of culture enrichment with PHA-storing organisms through application of a selective pressure, usually a “feast and famine” regime. Finally, the third step consists of PHA production, wherein the selected culture is fed with the fermented stream (FS) obtained in the acidogenic fermentation step, with an aim to reach the maximum PHA capacity of the culture.

The distribution profile of organic acids in the FS appears to depend on the type of feedstock used and the operating conditions of the acidogenic reactor (Carvalheira and Duque, 2021). Thus, by changing the operating conditions for acidogenic fermentation, such as the pH, retention time and organic loading rate (OLR), fermented products with different profiles can be obtained, mainly acetic, propionic and butyric acids (Bengtsson et al., 2008; Calero et al., 2018b; Carvalheira et al., 2018; Gouveia et al., 2017; Valentino et al., 2019). Laboratory studies using CW as a feedstock have shown that changes in the pH, and hydraulic and solid retention time produce streams differing in composition and consequently HV precursor content (Bengtsson et al., 2008; Calero et al., 2018b; Gouveia et al., 2017). These studies have indicated that increases in these parameters promote a shift from butyric acid to propionic acid production, favoring the production of HV precursors. Generally, an increase in OLR favors the production of VFA as more carbon becomes available. However, an adequate amount of carbon should be provided, because high OLR can lead to unstable operation and inhibit the microorganisms’ metabolism, owing to the presence of inhibitory substances (Carvalheira and Duque, 2021; Swiatkiewicz et al., 2021). The amount and the type of substrate fed to a system influence the metabolic pathways (e.g., butyric acid fermentation or propionic acid fermentation) and consequently the main acids produced, and can promote changes in the microbial community, thus contributing to changes in the acid distribution (Swiatkiewicz et al., 2021; Wainaina et al., 2020). Calero et al. (2018a, 2018b) have studied the effects of OLR on the production and distribution of VFA from CW, and observed a negative correlation between butyric and propionic acids: the production of butyric acid increases, and that of propionic acid decreases, with increasing OLR. Nevertheless, prior studies have focused on the effects of OLR on the yield and distribution of individual VFAs, but not on the PHA precursor content. Because modulating the HV content in the polymer can improve the thermal properties, studying the correlation between OLR and HV precursors and assessing the relationship between precursor content and polymer composition are crucial. Therefore, this work aimed at assessing the effects of OLR on the composition of the FS, and consequently on the HV precursor fraction, to produce and characterize tailored PHA by tuning the composition of the acidogenic fermentation stream. The produced polymers with different monomeric compositions were then characterized to assess their properties and potential applications.

Materials and methods

Three-stage pilot scale production of PHA

Experimental setup

The pilot scale setup for the production of PHA from CW by MMC consisted of a three reactor system: a 100 L upflow anaerobic sludge blanket (UASB) reactor–acidogenic reactor, a 200 L sequencing batch reactor (SBR)–culture selection reactor and a 60 L fed-batch reactor–production reactor.

Acidogenic reactors. The acidogenic fermentation of CW was performed in the UASB reactor, which was inoculated with 30 L of anaerobic granular sludge, which was harvested from a biogas production anaerobic digestion system treating brewery wastewater, and fed with CW. The CW was composed of lactose (78.4 wt%), proteins (13.6 wt%) and fats (1.2 wt%) (source: Lactogal–CW supplier). No additional nutrients were supplied to the reactor, because CW has been demonstrated to contain all nutrients required for the activity of acidogenic consortia (Duque et al., 2014). The UASB reactor was operated at 30 °C, and the pH was controlled between 4.50 and 5.00 for inhibition of methanogenic activity, through automatic addition of 5 M NaOH, a hydraulic retention time (HRT) of 1 d and uncontrolled sludge retention time. A superficial velocity was maintained at 4 $m.h^{-1}$ with a recirculation flow controlled at 3.03 $L.min^{-1}$. A relatively low organic loading rate (OLR) (5 $gCW.L^{-1}.d^{-1}$; 4.6 ± 0.1 $gCOD.L^{-1}.d^{-1}$; stage I) was applied to the UASB reactor during the first 4 days, to allow for the acclimation of granules to the CW feedstock. The OLR was subsequently varied between 10 and 25 $gCW.L^{-1}.d^{-1}$ (9.1 ± 0.7 to 25.1 ± 1.5 $gCOD.L^{-1}.d^{-1}$; Table 1). The OLR variations were aimed at not only tuning the FS composition—through adjustment of the fermentation product (FP) content of hydroxybutyrate/hydroxyvalerate (HB/HV) precursor, and targeting different monomeric ratios of HB/HV in the subsequently produced PHA polymer—but also maximizing FP productivity. The different precursor ratios enabled us to produce PHA differing in HB/HV content and identify the polymer with the best thermal properties for melt processing.

Selection reactors. For selection of a PHA-accumulating culture for PHA production, a 200 L SBR, with a working volume of 150 L was inoculated with aerobic sludge from a municipal wastewater treatment plant (Almada, Portugal) and operated under a feast and famine regime with uncoupled carbon and nitrogen availability, and fed with diluted FS. The operating conditions for the SBR reactor were adapted from those in a previous study of MMC PHA production from FS of CW (Oliveira et al., 2018, 2017).

Production reactor. The PHA production was performed in a fed-batch reactor of 60 L inoculated with sludge harvested from the SBR and fed with the FS produced in the UASB reactor after different production times, in pulse-wise mode, controlled by dissolved oxygen. The reactor was operated with no pH control and at controlled room temperature (23–25 °C). Dissolved oxygen and pH were continuously monitored. For the production of PHA with HV contents of 40 and 60 wt%, the FS was supplemented with valeric acid (an HV precursor). After the maximum PHA content in the cells was reached, the biological activity was stopped by quenching to pH 2–3 with sulfuric acid. Then the PHA was extracted and purified before polymer characterization. Extraction and purification were performed with a method based on non-organic solvents, thus resulting in extraction and purification yields of 85% and 95%, respectively. This method is licensed by Biotrend S.A. (Cantanhede, Portugal), and a patent application is pending.

Table 1
Summary of the operational stages applied to the UASB reactor.

Stage	Time (d)	OLR
I	0–4	5 $gCW.L^{-1}.d^{-1}$ (4.6 ± 0.1 $gCOD.L^{-1}.d^{-1}$)
II	5–39	10 $gCW.L^{-1}.d^{-1}$ (9.8 ± 1.6 $gCOD.L^{-1}.d^{-1}$)
III	40–75	20 $gCW.L^{-1}.d^{-1}$ (21.5 ± 2.3 $gCOD.L^{-1}.d^{-1}$)
IV*	76–80	30 $gCW.L^{-1}.d^{-1}$ (28.9 ± 1.7 $gCOD.L^{-1}.d^{-1}$)
V	81–123	20 $gCW.L^{-1}.d^{-1}$ (20.8 ± 4.2 $gCOD.L^{-1}.d^{-1}$)
VI	125–200	25 $gCW.L^{-1}.d^{-1}$ (25.1 ± 1.5 $gCOD.L^{-1}.d^{-1}$)

* This stage corresponds to the perturbation in the reactor.

Analytical methods

The chemical oxygen demand (COD) was determined with a Hach Lange kit (LCK 914; Hach-Lange, Germany). Total suspended solids (TSS) and volatile suspended solids (VSS) were determined according to standard methods (APHA/AWWA, 1995). Biogas composition (CH_4, CO_2, H_2, N_2 and O_2) was determined with a gas chromatograph equipped with a TCD detector and 50 m CP-Molsieve 5A and 25 m PoraBOND Q columns. Argon was used as the mobile phase (flow rate of 5 $mL.min^{-1}$), and the injection port and detector temperatures were 120 °C and 70 °C, respectively. Nutrient concentrations (i.e., ammonia and phosphorus) were determined through a colorimetric method with a segmented flow analyzer (Skalar San++, Skalar Analytical, the Netherlands). FP and lactose concentrations were determined by high performance liquid chromatography as described by Oliveira et al. (2018, 2017), with a Chromaster VWR Hitachi instrument equipped with both RI and UV (wavelength 210 nm) detectors, a Bio-Rad 125–0129 pre-column and an Aminex HPX-87H (Bio-Rad) column (0.01 M H_2SO_4 eluent, flow rate 0.6 $mL.min^{-1}$ and column temperature 60 °C). PHA content and composition were quantified through gas chromatography with a Bruker 430-GC instrument, as described by Lanham et al. (2013). The molecular weight and polydispersity index were determined with size exclusion chromatography, as described by Pereira et al. (2019).

PHA thermal characterization

The thermal properties of PHA were characterized for a preliminary assessment of potential applications in melt processing (extrusion, injection, thermoforming and coating for hot tack application). A rotational stress-controlled rheometer (ARG2, TA Instruments) was used to assess the softening point (temperature) of the produced PHA. Samples in powder form were loaded into the shearing geometry (parallel plates with diameter of 20 mm) pre-heated at 100 °C. Powders were compacted in the geometry with a removable metallic circular ring (to keep the powder in the geometry during the reduction of sample thickness) and application of a controlled normal force up to 12 N. Then the temperature was ramped to 200 °C at a rate of 5 °C/min, and the normal force was recorded. The thermal expansion of the shearing geometry was corrected during testing by maintaining a constant sample thickness. Differential scanning calorimetry (DSC) curves of PHBV samples (nearly 10 mg per sample) were measured with a Netzsch DSC200F3 instrument at a heating rate of ± 10 °C/min under nitrogen purging.

Calculations

The yield of FP in lactose ($Y_{FP/Lactose}$, $gCOD_{FP}.gCOD^{-1}_{Lactose}$) was determined with the following equation:

$$Y_{FP/Lactose} = \frac{FP_{out}}{Lactose_{in} - Lactose_{out}}$$

where FP_{out} corresponds to the concentration of FP in the reactor ($gCOD.L^{-1}$), and $Lactose_{in}$ and $Lactose_{out}$ correspond to the lactose concentrations in the feed and the reactor ($gCOD.L^{-1}$), respectively.

The acidification degree in the acidogenesis step was calculated as the ratio between the amount of FP produced (ΔFP, $gCOD_{FP}.L^{-1}$) and the total COD in the feed ($TCOD_{in}$, $gCOD.L^{-1}$):

$$\text{acidificationdegree } (\%) = \frac{\Delta FP}{TCOD_{in}} \times 100$$

FP volumetric productivity ($gCOD_{FP}.L^{-1}.d^{-1}$) was calculated by dividing the FP produced, converted to COD units, by the HRT (days).

The feast and famine ratio ($h.h^{-1}$) was determined as the ratio of the durations of the feast and famine phases. The PHA content in the biomass was determined in terms of VSS (PHA (wt.%) = 100 × (PHA/VSS), $gPHA.gVSS^{-1}$). The active biomass concentration (X, $g.L^{-1}$) was calculated according to the difference between VSS and PHA concentrations ($g.L^{-1}$). To convert X to Cmol and COD, we used the generic formula $C_5H_7NO_2$, and conversion factors of 44.2 $Cmmol_X.g_X^{-1}$ and 1.41 $gCOD_X.g_X^{-1}$, respectively. The FP consumption rate ($gCOD.gCOD_X^{-1}.h^{-1}$) and PHA storage rate ($gCOD_{PHA}.gCOD_X^{-1}.h^{-1}$) were determined on the basis of the slope of the linear regression of total FP and PHA specific concentrations, respectively, plotted over time. The PHA storage yield ($gCOD_{PHA}.gCOD_{FP}^{-1}$) was calculated as the ratio between the specific PHA storage rate and specific FP consumption rate. PHA productivity ($g_{PHA}.L^{-1}.d^{-1}$) was determined according to the amount of PHA produced per unit accumulation reactor volume and per unit time.

Results and discussion

Pilot scale performance

Acidogenic fermentation

The UASB reactor was operated for 200 days under different OLR (corresponding to six stages) to promote the conversion of CW into FP. The concentrations of TSS and VSS in the effluent of the UASB were 8.9 ± 2.0 g/L and 7.6 ± 1.7 g/L, respectively. The different operating conditions applied to the UASB reactor resulted in various FS compositions and productivity levels, thus allowing us to determine the conditions for obtaining the desired HV precursor content (10, 20 or 30 wt%). According to general knowledge, lactic acid (H.Lact), acetic acid (H.Acet), isobutyric acid (H.isoBut) and butyric acid (H.But) were considered HB precursors, and propionic acid (H.Prop), isovaleric acid (H.isoVal), valeric acid (H.Val) and ethanol (EtOH) were considered HV precursors (Duque et al., 2014). Additionally, because hexanoic acid (H.Hex) was consistently detected in the UASB reactor's FS, a batch test using this organic acid as substrate was performed to identify its metabolic pathway. Because H.Hex produced HB monomers (data not shown), this acid was considered an HB precursor.

The successive OLR increase from 4.6 ± 0.1 $gCOD.L^{-1}.d^{-1}$ (stage I) to 20.8 ± 4.2 $gCOD.L^{-1}.d^{-1}$ (stage V) allowed for a gradual acclimation of the culture to CW, as reflected by the increase in FP concentration from 3.9 ± 1.6 $gCOD.L^{-1}$ (stage I) to 18.7 ± 2.0 $gCOD.L^{-1}$ (stage V) (Fig. 1), as well as the inhibition of methanogenic activity (indicated by the decrease in methane content in the gas; data not shown). At day 76, a perturbation in the system occurred, which led to an OLR increase to 28.9 ± 1.7 $gCOD.L^{-1}.d^{-1}$ (stage IV). However, this OLR was not maintained because it caused a substantial increase in gas production, which destabilized the hydrodynamic balance of the reactor, thereby causing a loss of anaerobic granules through the effluent outlet. Nevertheless, the FS obtained during this short period was used for the production of PHA with approximately 30 wt% HV. This perturbation at high OLR has also been observed by Matos et al. (2021) during

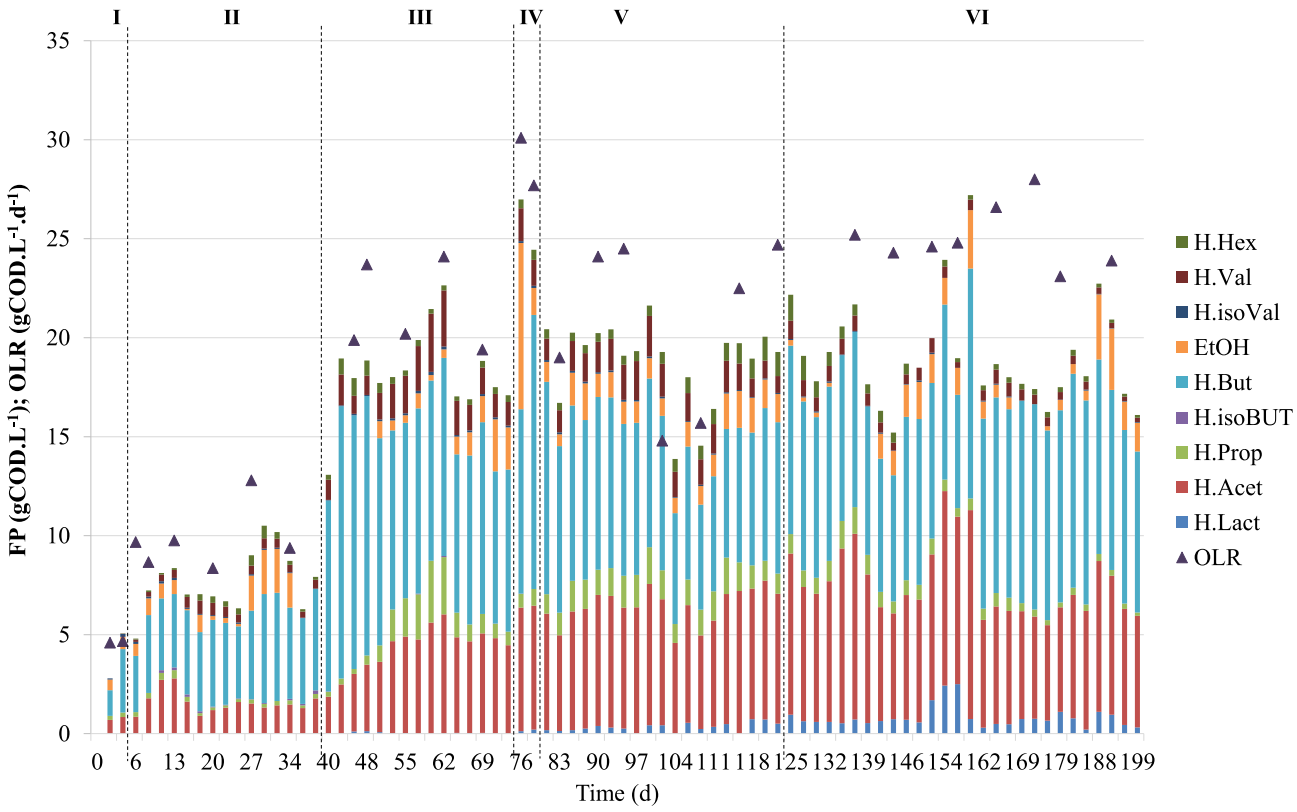

Fig. 1. Profile and concentration of the obtained fermentation products (FP) with UASB reactor operation under different organic loading rates (OLR).

UASB operation treating fruit pulp. To re-stabilize the reactor, we reverted the OLR to the previous value (20.8 ± 4.2 $gCOD.L^{-1}.d^{-1}$; stage V), and then, to increase the FP productivity, increased it to 25.1 ± 1.5 $gCOD.L^{-1}.d^{-1}$ (stage VI). However, this increase did not significantly affect the FP productivity, thus resulting in a similar FP concentration (18.6 ± 2.7 $gCOD.L^{-1}$) to that in previous stages, at an OLR of approximately 20 $gCOD.L^{-1}.d^{-1}$ (18.1–18.7 $gCOD.L^{-1}$) (Table 2). The highest OLR applied was similar to that used to produce VFAs at pilot scale by using fruit pulp waste (Carvalheira et al., 2018) or waste activated sludge (Morgan-Sagastume et al., 2011).

Throughout the operation, and independently of the conditions imposed, lactose was completely consumed, and the rate of FP production reached 18.5 ± 0.3 $gCOD_{FP}.L^{-1}.d^{-1}$ when stable FP production was observed (stages III, V and VI). The fluctuations observed in FP concentrations at each stage were associated with the variation in OLR (Fig. 1). The productivity was in the same range as or even higher (10.0–17.8 $gCOD_{FP}.L^{-1}.d^{-1}$) than that previously reported at pilot scale under a similar OLR (Carvalheira et al., 2018; Morgan-Sagastume et al., 2011). We obtained higher productivity than that in other studies using CW at laboratory scale. However, those studies used a lower OLR (13.5–15.9 $gCOD_{FP}.L^{-1}.d^{-1}$) at the same HRT, thus explaining the lower productivity (10–14 $gCOD_{FP}.L^{-1}.d^{-1}$) (Duque et al., 2014; Gouveia et al., 2017).

Throughout operation, the yield of FP in lactose ($Y_{FP/Lactose}$) was consistently higher than 0.67 $gCOD_{FP}.gCOD^{-1}_{Lactose}$, and a maximum of 0.97 $gCOD_{FP}.gCOD^{-1}_{Lactose}$ and a global yield of 0.87 ± 0.12 $gCOD_{FP}.gCOD^{-1}_{Lactose}$ were achieved. The acidification degree varied between 60% and 84%, corresponding to an average of 77 ± 10% (80 ± 5% considering the period of stable FP production) (Table 2), and was not affected by the OLR increase, in contrast to observations in other studies using CW as feedstock (Calero et al., 2018a, 2018b). The difference between $Y_{FP/Lactose}$ and the acidification degree might have been due to the proteins and lipids present in the CW (composing approximately 14 wt% and 1 wt% of the CW, respectively), which might also contribute to acetic, propionic and butyric acid production (Hassan and Nelson, 2012). The obtained acidification degree was similar to (74–84% using fruit pulp) or higher than (15–31% using waste activated sludge and/or the organic fraction of municipal solid waste) the values observed in other pilot scale studies (Carvalheira et al., 2018; Matos et al., 2021; Morgan-Sagastume et al., 2015; Valentino et al., 2019, 2018). These differences in the acidification degree might relate to the type, composition and readily biodegradable organic matter content of the different feedstocks, thereby affecting the hydrolysis/acidification step. Because CW is a sugar-rich substrate (Duque et al., 2014), the FP conversion occurs more readily than that for complex substrates with low biodegradability; consequently, a higher acidification can be obtained. Indeed, in Moretto's study (2020) a higher acidification degree was observed when the feedstock was subjected to a pre-treatment increasing the content of soluble organic matter. The global yield was in the same range as those in previous studies at laboratory scale, using substrates rich in sugars (CW: 0.65–0.74 $gCOD_{FP}.gCOD^{-1}_{Sugar}$ (Duque et al., 2014) and 0.74–0.87 $gCOD.gCOD^{-1}$ (Bengtsson et al., 2008); molasses: 0.8 $gCOD_{FP}.gCOD^{-1}_{Sugar}$ (Duque et al., 2014)).

The different OLRs applied to the UASB resulted in varying FS compositions and consequently affected the amounts of HV precursors obtained, as observed in other studies (Bengtsson et al., 2008; Carvalheira et al., 2018; Gouveia et al., 2017; Valentino et al., 2019). In all conditions, H.Acet and H.But, both HB precursors, were the main compounds produced, composing at least 70% of the total FP (gCOD basis). This high content of H.Acet and H.But was also obtained when glucose, lactose or CW was used as a substrate (Davila-Vazquez et al., 2008). Because of the variations in H.Prop, H.Val and EtOH production throughout the operation, the HV precursors varied between 9 and 19 wt% during the stable production of FP, thus allowing for the production of PHA with different HV content

Table 2
Performance of the acidogenic reactor under different operational conditions.

Stage	OLR ($gCOD.L^{-1}.d^{-1}$)	FP productivity ($gCOD_{FP}.L^{-1}.d^{-1}$)	$Y_{FP/Lactose}$ ($gCOD_{FP}.gCOD^{-1}_{Lactose}$)	Acidification degree (%)	HV precursors (wt. %)
I	4.6 ± 0.1	3.9 ± 1.6	0.67 ± 0.41	60 ± 34	20
II	9.8 ± 1.6	7.8 ± 1.3	0.94 ± 0.19	83 ± 8	16
III	21.5 ± 2.3	18.1 ± 2.2	0.90 ± 0.15	82 ± 19	19
IV*	28.9 ± 1.7	25.5 ± 1.8	0.93 ± 0.07	88 ± 1	33
V	20.8 ± 4.2	18.7 ± 2.0	0.97 ± 0.13	84 ± 6	18
VI	25.1 ± 1.5	18.6 ± 2.7	0.89 ± 0.10	75 ± 10	9

* This stage corresponds to the perturbation in the reactor, and the obtained FS was used to produce PHA with approximately 30 wt% HV.

grades. The production of H.Lact was observed only during the last conditions applied (stages IV to VI), but in small amounts (1–4%), in contrast to Gouveia's findings (2017), in which H.Lact was the main compound produced independently of the applied pH. This discrepancy might be related to different reactor configurations or inocula used (Duque et al., 2014). The results suggested that the microbial culture was enriched in organisms that predominantly performed two metabolic pathways: fermentation of H.Acet and H.But.

The obtained results indicated that the increase in OLR affected the production of HV precursors, mainly when the OLR increased from approximately 20 to 25 $gCOD.L^{-1}.d^{-1}$ (from stage V to VI), where the variation in HV precursor content was more prominent. In contrast, only a slight increase in HV precursors was observed when the OLR changed from 9.8 to 21.5 $gCOD.L^{-1}.d^{-1}$ (from stage II to III, Table 2).

The decrease in HV precursors is likely to relate to the increase in hydrogen (H_2) content in the produced gas stream. Indeed, a correlation between these parameters was observed (Fig. 2). The content of H.Prop and H.Val, the main HV precursors, decreased with increasing H_2 (H.Prop = -0.19.H_2 + 0.06; H.Val = -0.20.H_2 + 0.06). H_2 has been reported to be produced by the metabolic pathways of acetic and butyric acid fermentation, whereas propionic acid fermentation is associated with little or no H_2 production (Chu et al., 2008; Cohen et al., 1984; Moreira et al., 2017). These findings are consistent with our findings, because H_2 production increased when the content of HB precursors increased, and composed more than 80 wt% (gCOD basis) of the total FP, whereas the HV precursors decreased. These results demonstrated that H_2 production might potentially be used as an indicator of the dynamics of HV/HB precursor production.

PHA production

An SBR system was operated for 139 days under a feast and famine regime. The objective was to select an MMC culture enriched in PHA-storing organisms to produce PHA with differing HV content. The FS produced during the UASB stage III was used in SBR acclimation, and the FS produced during UASB stages V and VI was used for SBR maintenance and PHA production. Because nutrients were not supplemented in the UASB feedstock, the content of ammonia and phosphorus in the FS was low, corresponding to a C:N:P ratio of 100:0.01:0.37 on a mass basis (100:0.09:0.43 on a molar basis). Therefore, the selection reactor was able to operate under uncoupled carbon and nitrogen availability, thus producing PHA in the absence of nutrients, and resulting in high PHA yield and productivity (Oliveira et al., 2017).

During the operation, the feast to famine ratio (F/f) was < 0.2, a threshold demonstrated to ensure effective selective pressure for PHA accumulating microorganisms (Duque et al., 2014; Valentino et al., 2019). Indeed, the selected culture demonstrated favorable PHA accumulation, achieving a maximum PHA storage yield ($Y_{PHA/FP}$) of 0.72 ± 0.08 $gCOD_{PHA}.gCOD^{-1}_{FP}$ under an OLR of 5.6 ± 0.5 $gCOD_{FP}.L^{-1}.d^{-1}$. This PHA storage yield was among the highest reported at pilot scale (Matos et al., 2021; Moretto et al., 2020; Valentino et al., 2019).

The culture selected on the SBR was used as an inoculum for the PHA production fed-batch reactor. FS produced in stages VI and V was used to produce PHA with 11 wt% HV and 20 wt% HV, respectively. As described above (section 3.1.1), the FS obtained during the system perturbation (stage IV) was used to produce PHA with 28 wt% HV. Additionally, PHAs with two higher HV grades (approximately 36 and 63 wt% HV) were produced by supplementation of the FS from stage VI with additional HV precursors (valeric acid) to obtain an HV precursor content of 40 and 60 wt%. The results from PHA production indicated that the HV content in the polymer was directly proportional to the HV precursors in FS (Fig. 3), thereby supporting the prior assumptions of the HV fraction prediction in this study. Moreover, this correlation indicated the feasibility of producing tailored PHA by modulating FS composition or precursor supplementation. This predictability of PHA composition has also been observed in a previous study using CW, which has obtained streams with different composition through changing the pH (Gouveia et al., 2017). Both studies indicated the ability to manipulate the HV content of the PHA through the production of FSs with different compositions, thus indicating the feasibility of controlling polymer composition. In addition, the re-stabilization of the HV precursors in the FS after the system perturbation (see section 3.1.1) also indicated the feasibility of modulating the polymer composition.

During all PHA production assays, and independently of HV content, FP were consumed linearly, with an average global consumption rate of 0.54 ± 0.14 $gCOD.gCOD^{-1}_X.h^{-1}$ (0.46 ± 0.13 $Cmol.Cmol^{-1}_X.h^{-1}$). This value was within the ranges reported in other studies using FS of CW (0.42–0.45 $Cmol.Cmol^{-1}_X.h^{-1}$) (Duque et al., 2014; Oliveira et al., 2017).

Independently of the content of HV precursors in FS (9–33 wt%), an average PHA content of 50 ± 11 wt% (VSS basis) was obtained, which was within the ranges reported in other pilot studies (39–52 wt%) (Chakravarty et al., 2010; Moretto et al., 2020; Valentino et al., 2020, 2019, 2018). For the PHA with HV monomeric fractions of 36 wt% HV and 63 wt% HV, intracellular PHA content of 60 and 51 wt%, respectively, was obtained. The PHA storage yield was independent of the HV content (Table 3), with a global yield of 0.76 ± 0.14 $gCOD_{PHA}.gCOD^{-1}_{FP}$, a value similar to that obtained in the selection stage (0.72 ± 0.08 $gCOD_{PHA}.gCOD^{-1}_{FP}$). Moreover, a global PHA storage rate of 0.56 ± 0.15 $gCOD_{PHA}.gCOD^{-1}_X.h^{-1}$ was obtained. The PHA yield was consistent with the values obtained in other studies (up to 0.57 $gCOD_{PHA}.gCOD^{-1}$ (Valentino et al., 2020, 2019, 2018); 0.69 ± 0.15 $gCOD_{PHA}.gCOD^{-1}$ (Morgan-Sagastume et al., 2020)) but lower than that obtained by Matos et al. (2021) (0.98 $gCOD_{PHA}.gCOD^{-1}$). Furthermore, the PHA storage rate was comparable to that obtained in Valentino's studies (2019, 2018) (up to 0.46 $gCOD_{PHA}.gCOD^{-1}_X.h^{-1}$) but lower than that observed by Matos et al. (2021) (1.01 $gCOD_{PHA}.gCOD^{-1}_X.h^{-1}$). The lower yield and rate might relate to the feeding strategy, given that continuous feeding was applied in Matos' study (2021), thus avoiding the consumption of PHA during the assay that might occur with a pulse-wise feeding strategy.

The PHA volumetric productivity in the production assays varied between 7.3 and 8.0 $g_{PHA}.L^{-1}.d^{-1}$, with an average productivity of 7.8 ± 0.3 $g_{PHA}.L^{-1}.d^{-1}$ (Table 3). These values were within the ranges

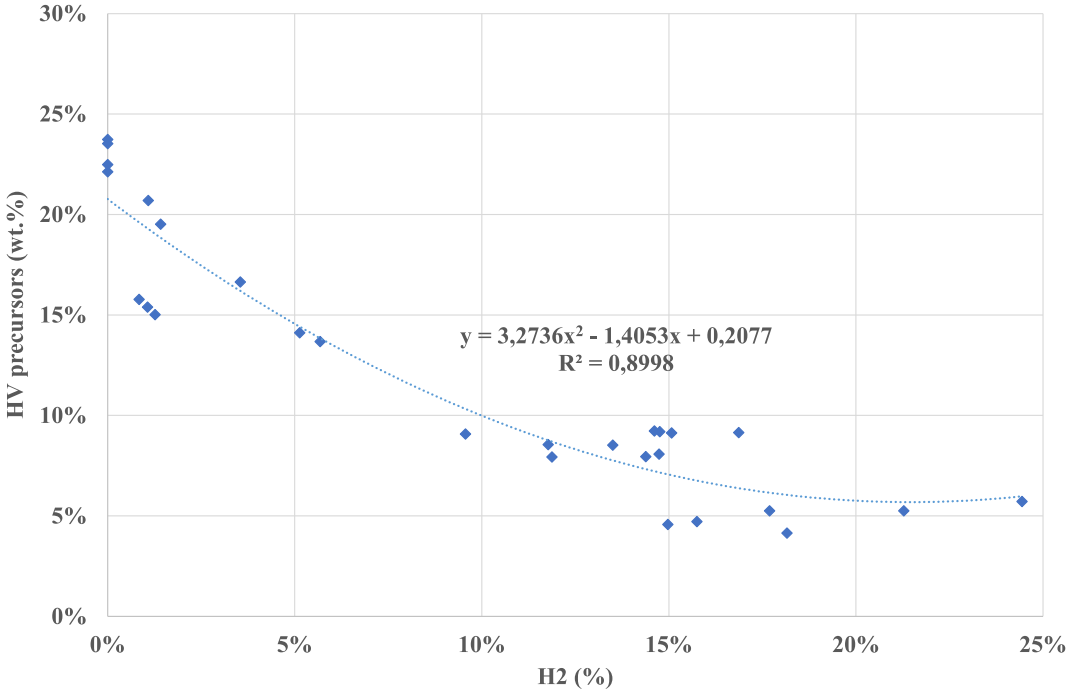

Fig. 2. Correlation between HV precursors and the percentage hydrogen content in the reactor outlet gas stream.

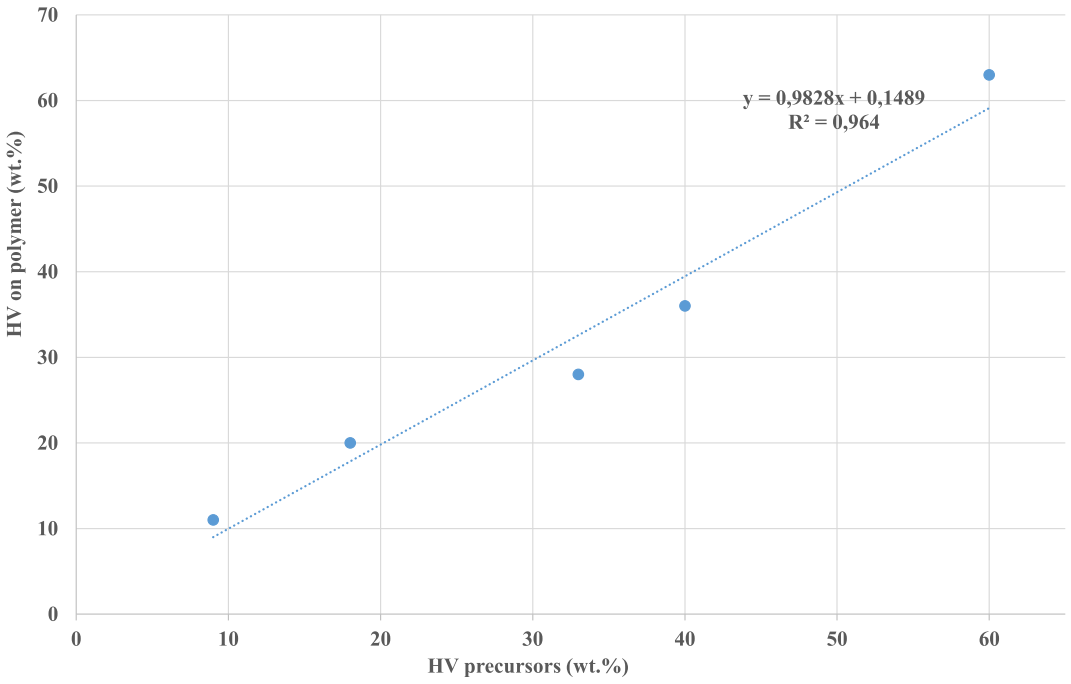

Fig. 3. HV content produced in PHA production assays as a function of the HV precursor content of the FS.

reported in other pilot studies (8.1–11.8 $g_{PHA}.L^{-1}.d^{-1}$) (Matos et al., 2021; Valentino et al., 2019, 2018). The independence of the reactor's performance from the type of PHA produced reflected the robustness of the process, thus representing an advantage in PHA production at large scale.

Overall, the production of 1 kg of PHA (corresponding to 1.73 kgCOD) required 11.9 kg of CW, thereby resulting in a global yield of 0.08 $kgPHA.kgCW^{-1}$ (0.15 $kgCODPHA.kgCW^{-1}$; 0.16 $kgCOD-PHA.kgCOD^{-1}$), and a conversion efficiency of approximately 15% was achieved. Because the carbon fed into the reactors was also used for other processes (culture growth and gas production), the low conversion efficiency was justified.

The accumulation assays using HV precursor supplementation indicated the feasibility of producing tailored PHA with different grades of HV by simply supplementing the feedstock during the PHA production assays. This aspect is advantageous for the PHA production industry, because it allows for production of PHA with the desired composition for a given final application, without the time consuming requirement

Table 3
PHA storage yield and productivity for differing HV content.

HV (wt.%)	$Y_{PHA/FP}$ ($gCOD_{PHA}.gCOD_{FP}^{-1}$)	PHA productivity ($g_{PHA}.L^{-1}.d^{-1}$)
11 ± 2	0.74 ± 0.06	7.9 ± 2.6
20 ± 2	0.72 ± 0.22	7.8 ± 1.5
28 ± 3	0.79 ± 0.08	7.7 ± 0.6
36[a]	0.75	7.3
63[a]	0.78	8.0

[a] Standard deviation were not determined, because only one assay was performed.

to select new cultures. Generally, the results obtained in acidogenic fermentation and PHA production suggested that the production of tailored PHA is viable through tuning the composition of the FS with the desired ratio of HB:HV precursors.

The produced PHA polymer had molecular weights between 482 and 551 kDa, and a polydispersity index between 1.77 and 3.46, values in the same range as those for the PHA produced by MMC by using wastes as a feedstock (220–547 kDa) (Duque et al., 2014; Matos et al., 2021; Morgan-Sagastume et al., 2020). Moreover, the PHA composition after extraction was similar to that determined in the final of the accumulation assays, thus indicating that the extraction method did not affect the PHA composition/characteristics. Because the molecular weight, polydispersity index and polymer composition affect the thermal properties and consequently the applications of the polymer, our study of the thermal behavior of the different polymers produced allowed us to identify the best composition to limit thermal degradation and achieve good crystallization after processing (section 3.2).

PHA thermal behavior

Fig. 4 shows the temperature dependence of the normalized normal force (with respect to the initial normal force $N_{100°C}$ set to 12 N at 100 °C) for the five PHAs produced with differing HV content. The normalized normal forces $N/N_{100°C}$ decreased after a range of temperatures was reached. This decrease indicated the softening of the materials associated with the glass transition regime, followed by the subsequent melting of the crystalline phases. The rate of the decrease in $N/N_{100°C}$, as well as the temperature range over which this decrease occurred, was dependent on the HV content.

The temperature at which half the sample elasticity (quantified by the normal force) is reached is defined as T_n, which was determined graphically (Fig. 4). The values of T_n (reported in Table 4 for all samples) indicated that softening occurred at lower temperatures when the HV content increased, with the exception of the PHBV containing 60 wt%. This finding was expected, because the melting temperature of PHBV is known to decrease from 179 °C to 75 °C when the HV content increases from 0 to 40% HV. For higher HV content, the melting temperature rises to 108 °C (Doi, 1990).

Overall, the T_n data indicated that the softening and partial crystal melting necessary for a hot tack application or thermoforming can be achieved at temperatures as low as 120–140 °C if PHBV containing at least 30 wt% HV is used.

Fig. 5 shows the DSC curves recorded during the first heating of powder materials. Qualitatively similar curves were observed for PHBV produced from CW at laboratory scale with 18 mol% HV content and tested under similar calorimetric conditions (Hilliou et al., 2016b). Among the various peaks resolved in the DSC curves plotted in Fig. 5, the peaks at the highest temperatures were of interest. These peaks corresponded to the melting of crystals rich in HB units, which are more heat resistant. The melting temperature of these crystals is reported as T_m in Table 4, and the temperature T_c indicates the end of the melting process for these crystals. Therefore, T_c can be considered the temperature at which the PHBV is fully in the molten state.

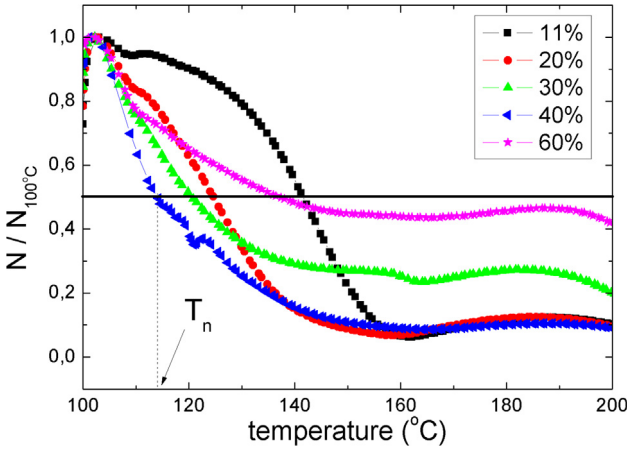

Fig. 4. Temperature dependence of the normalized normal force $N/N_{100°C}$ for all PHBV samples with varying HV content, indicated in wt.% in the legend. T_n is the temperature at which the sample elasticity decreased by 50%, indicated by the horizontal line.

The data in Table 4 suggested that the PHBV with 30 wt% HV exhibited the smallest T_m and T_c. As described earlier, a minimum T_m has been reported in the literature for 40 wt% HV (Doi, 1990). The overall DSC data confirmed the conclusions drawn from the thermorheological analysis in Fig. 4, indicating that 30 wt% HV composition was the best candidate for applications requiring the lowest processing temperature to limit the thermal degradation of the biopolyester. However, this conclusion is in opposition with by other features of the DSC curves of PHBV samples containing more HV monomers. For those samples, the melting process at T_m was much less than the melting processes occurring at lower temperatures. Consequently, the corresponding enthalpies were smaller, and most of the material actually melted at temperatures below T_c. Indeed, peaks with larger amplitudes were found below 100 °C for samples with 40 and 60 wt% HV. These peaks indicated the melting of HV crystals, which melted separately from HB-rich crystals. This finding was a characteristic of either the block copolymer nature of the produced PHBV or the blending of random copolymers with different HV content (Laycock et al., 2014b, 2014a). These peaks explained the broader softening processes observed in the rheological tests at T_n (Fig. 4) and therefore confirmed that PHBV with 40 wt% HV may serve as an alternative candidate for thermal processing.

Fig. 6 presents the DSC curves measured during the cooling of samples immediately after the heating of the powders. Curves for PHBV containing more than 20 wt% HV were featureless, as expected because of the low crystallization kinetics of HV crystals (Bloembergen et al., 1986).

For samples with 11 and 20 wt% HV, the crystallization of HB crystals was measured during cooling. The corresponding curves indicated earlier crystallization with lower HV content, thus suggesting that this PHBV might be easiest to post process after melting, because all other samples would require much longer times and colder temperatures to reach shape stability and full crystallization after stretching or laminating. This aspect is illustrated in Fig. 7, which displays the DSC curves measured during the second heating following the cooling shown in Fig. 6.

All samples except those with an HV content of 60 wt% exhibited a cold crystallization process, which resulted in the melting of the HB crystals, which resolved as a peak at the highest temperatures. The corresponding peak melting temperature T_{m2} and complete melting temperature T_{c2} (Table 4) confirmed that full melting occurred at lower temperatures when the HV content was increased from 11 to 30 wt %. Interestingly, a single glass transition process was observed just

Table 4
Softening temperature T_n, melting temperature T_m of HB crystals, complete molten temperature T_c and crystallization temperature T_{cc} for PHBV polymers with varying HV content, studied with a heating rate of 10 °C/min followed by a cooling rate of −10 °C/min. T_{m2} and T_{c2} are the HB crystals and complete melting temperatures, respectively, measured after the cooling of samples.

HV content (wt.%)	T_n (°C)	T_m (°C)	T_c (°C)	T_{cc} (°C)	T_{m2} (°C)	T_{c2} (°C)
11	141.7 ± 0.5	159 ± 1	170.6 ± 1	54 ± 1	147.5 ± 1	160 ± 1
20	124.6 ± 0.6	159 ± 1	169.6 ± 1	44 ± 3	142.0 ± 1.5	153 ± 1
30	120.8 ± 0.5	157 ± 1	167.7 ± 1	–	139 ± 2.5	148 ± 1
40	114.2 ± 0.5	163.8 ± 1	175 ± 2	–	153.5 ± 0.5	166 ± 2
60	136.4 ± 0.8	158 ± 1	167.5 ± 1	–	–	–

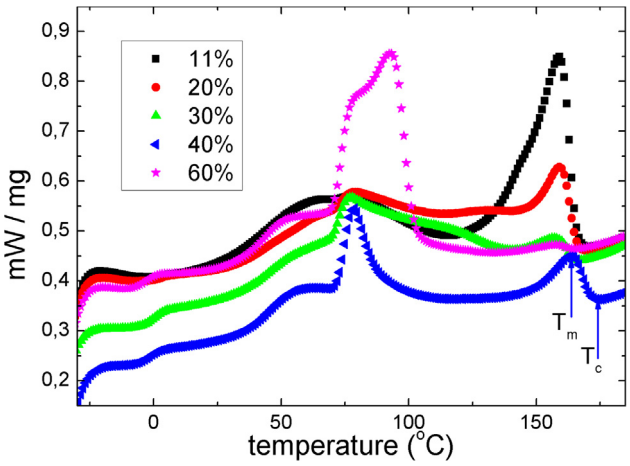

Fig. 5. DSC curves of PHBV samples, with HV content as specified in the legend. The arrows indicate the graphical determination of the melting temperature T_m of HB crystals and complete molten temperature T_c.

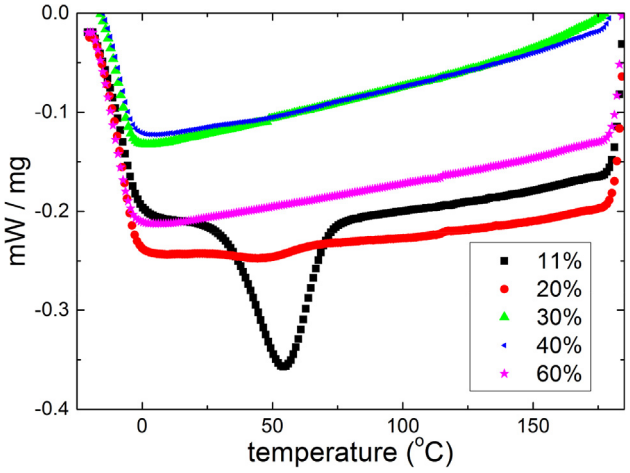

Fig. 6. DSC curves recorded during the cooling of PHBV samples, with HV content as specified in the legend.

below 0 °C in the traces in Fig. 7. This finding indicated that either miscible blends of PHBV or random PHBV copolymers were fermented, rather than copolymers with distinct HV and HB blocks. PHBV fractionation and additional polymer characterization would be required to confirm this possibility (Laycock et al., 2014b, 2014a). However, the data regarding thermal properties presented in Figs. 4–7 confirmed that PHBV with tailored HV content was produced, which exhibited differing thermal properties. Additional rheological testing and extrusion trials should be performed to confirm that a content of 30 wt% HV is optimal to process materials at lower temperatures while retaining acceptable crystallization kinetics, because no clear correlation

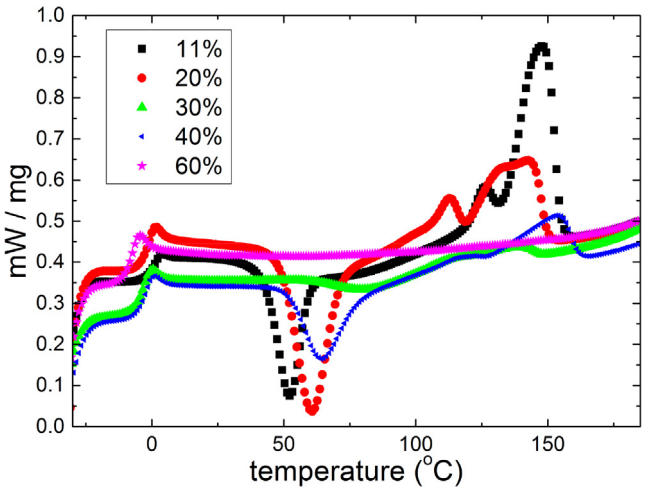

Fig. 7. DSC curves recorded during the second heating of PHBV samples, with HV content as specified in the legend.

between the HV content and the melt rheology or processability has been inferred from earlier studies on PHBV with comparable molecular masses (Hilliou et al., 2016a; Ramkumar and Bhattacharya, 1998).

Conclusions

This study demonstrated the feasibility of producing tailored PHA by controlling the operating conditions of acidogenic fermentation to produce a stream with a specific HV precursor content. The changes in OLR allowed us to obtain different FP compositions and consequently produce PHA with differing HB/HV content. Moreover, the supplementation of FS with HV precursors only during the accumulation step allowed us to produce PHA with high HV content without a need to reinoculate/restart the reactor for each desired polymer, thus demonstrating the robustness of the process. Consequently, the thermal properties of produced PHA can be tuned. Our findings confirmed the production of copolymers with differing HV content and probably a random structure. An optimum was found for an HV content of approximately 20–30 wt%, which provides a balance between melting or softening at lower temperatures, thus limiting thermal degradation and enabling sufficient crystallization after post processing.

Overall, the results obtained in this study indicated the feasibility of designing, producing and characterizing tailored PHA polymers for use in melt processing.

CRediT authorship contribution statement

Mónica Carvalheira: Conceptualization, Methodology, Investigation, Supervision, Writing – original draft. **Loic Hilliou:** Conceptualization, Investigation, Writing – original draft. **Catarina S.S. Oliveira:** Conceptualization, Methodology, Investigation, Supervision,

Writing – review & editing. **Eliana C. Guarda:** Investigation. **Maria A. M. Reis:** Supervision, Funding acquisition, Conceptualization, Writing – review & editing.

Declaration of Competing Interest

The authors declare that they have no known competing financial interests or personal relationships that could have appeared to influence the work reported in this paper.

Acknowledgements

The authors acknowledge financial support from the European project YPack (H2020-SFS-35-2017) and additional financial support from the FCT–Fundação para a Ciência e a Tecnologia, I.P. under the framework of Strategic Funding grant UID/CTM/50025/2020.

Funding

This work was financed by national funding from FCT–Fundação para a Ciência e a Tecnologia, I.P., in the scope of projects UIDP/04378/2020 and UIDB/04378/2020 of the Research Unit on Applied Molecular Biosciences–UCIBIO and project LA/P/0140/2020 of the Associate Laboratory Institute for Health and Bioeconomy–i4HB.

References

APHA/AWWA, 1995. Standard Methods for the Examination of Water and Wastewater. Port City Press, Balt.

Bengtsson, S., Hallquist, J., Werker, A., Welander, T., 2008. Acidogenic fermentation of industrial wastewaters: effects of chemostat retention time and pH on volatile fatty acids production. Biochem. Eng. J. 40, 492–499. https://doi.org/10.1016/j.bej.2008.02.004.

Bloembergen, S., Holden, D.A., Hamer, G.K., Bluhm, T.L., Marchessault, R.H., 1986. Studies of composition and crystallinity of bacterial poly(β-hydroxybutyrate-co-β-hydroxyvalerate). Macromolecules 19, 2865–2871. https://doi.org/10.1021/ma00165a034.

Calero, R.R., Iglesias-Iglesias, R., Kennes, C., Veiga, M.C., 2018. Organic loading rate effect on the acidogenesis of cheese whey: a comparison between UASB and SBR reactors. Environ. Technol. 39, 3046–3054. https://doi.org/10.1080/09593330.2017.1371796.

Calero, R.R., Lagoa-Costa, B., del Fernandez-Feal, M.M., C., Kennes, C., Veiga, M.C.,, 2018. Volatile fatty acids production from cheese whey: influence of pH, solid retention time and organic loading rate. J. Chem. Technol. Biotechnol. 93, 1742–1747. https://doi.org/10.1002/jctb.5549.

Carvalheira, M., Cassidy, J., Ribeiro, J.M., Oliveira, B.A., Freitas, E.B., Roca, C., Carvalho, G., Oehmen, A., Reis, M.A.M., 2018. Performance of a two-stage anaerobic digestion system treating fruit pulp waste: The impact of substrate shift and operational conditions. Waste Manag. 78, 434–445. https://doi.org/10.1016/j.wasman.2018.06.013.

Carvalheira, M., Duque, A.F., 2021. From Food Waste to Volatile Fatty Acids towards a Circular Economy, in: Fermentation - Processes, Benefits and Risks [Working Title]. https://doi.org/10.5772/intechopen.96542.

Chakravarty, P., Mhaisalkar, V., Chakrabarti, T., 2010. Study on poly-hydroxyalkanoate (PHA) production in pilot scale continuous mode wastewater treatment system. Bioresour. Technol. 101, 2896–2899. https://doi.org/10.1016/j.biortech.2009.11.097.

Chu, C.F., Li, Y.Y., Xu, K.Q., Ebie, Y., Inamori, Y., Kong, H.N., 2008. A pH- and temperature-phased two-stage process for hydrogen and methane production from food waste. Int. J. Hydrogen Energy 33, 4739–4746. https://doi.org/10.1016/j.ijhydene.2008.06.060.

Cohen, A., Jm, V., Zoetemeyer, R., Breure, A., 1984. Main characteristics and stoichiometric aspects of acidogenesis of soluble carbohydrate containing w. Process Biochem. 19.

Cunha, M., Fernandes, B., Covas, J.A., Vicente, A.A., Hilliou, L., 2016. Film blowing of PHBV blends and PHBV-based multilayers for the production of biodegradable packages. J. Appl. Polym. Sci. 133. https://doi.org/10.1002/app.42165.

Davila-Vazquez, G., Alatriste-Mondragón, F., de León-Rodríguez, A., Razo-Flores, E., 2008. Fermentative hydrogen production in batch experiments using lactose, cheese whey and glucose: Influence of initial substrate concentration and pH. Int. J. Hydrogen Energy 33, 4989–4997. https://doi.org/10.1016/j.ijhydene.2008.06.065.

Doi, Y., 1990. Microbial polyesters. VCH, New York.

Duque, A.F., Oliveira, C.S.S., Carmo, I.T.D., Gouveia, A.R., Pardelha, F., Ramos, A.M., Reis, M.A.M., 2014. Response of a three-stage process for PHA production by mixed microbial cultures to feedstock shift: Impact on polymer composition. N. Biotechnol. 31, 276–288. https://doi.org/10.1016/j.nbt.2013.10.010.

Gouveia, A.R., Freitas, E.B., Galinha, C.F., Carvalho, G., Duque, A.F., Reis, M.A.M., 2017. Dynamic change of pH in acidogenic fermentation of cheese whey towards polyhydroxyalkanoates production: Impact on performance and microbial population. N. Biotechnol. 37, 108–116. https://doi.org/10.1016/j.nbt.2016.07.001.

Gurieff, N., Lant, P., 2007. Comparative life cycle assessment and financial analysis of mixed culture polyhydroxyalkanoate production. Bioresour. Technol. 98, 3393–3403. https://doi.org/10.1016/j.biortech.2006.10.046.

Hassan, A.N., Nelson, B.K., 2012. Invited review: Anaerobic fermentation of dairy food wastewater. J. Dairy Sci. 95, 6188–6203. https://doi.org/10.3168/jds.2012-5732.

Hilliou, L., Machado, D., Oliveira, C.S.S., Gouveia, A.R., Reis, M.A.M., Campanari, S., Villano, M., Majone, M., 2016. Impact of fermentation residues on the thermal, structural, and rheological properties of polyhydroxy(butyrate-co-valerate) produced from cheese whey and olive oil mill wastewater. J. Appl. Polym. Sci. 133, 42818. https://doi.org/10.1002/app.42818.

Hilliou, L., Teixeira, P.F., Machado, D., Covas, J.A., Oliveira, C.S.S., Duque, A.F., Reis, M.A.M., 2016. Effects of fermentation residues on the melt processability and thermomechanical degradation of PHBV produced from cheese whey using mixed microbial cultures. Polym. Degrad. Stab. 128, 269–277. https://doi.org/10.1016/j.polymdegradstab.2016.03.031.

Keskin, G., Kızıl, G., Bechelany, M., Pochat-Bohatier, C., Öner, M., 2017. Potential of polyhydroxyalkanoate (PHA) polymers family as substitutes of petroleum based polymers for packaging applications and solutions brought by their composites to form barrier materials. Pure Appl. Chem. 89, 1841–1848. https://doi.org/10.1515/pac-2017-0401.

Lanham, A.B.A.B., Ricardo, A.R.A.R., Albuquerque, M.G.E.M.G.E., Pardelha, F., Carvalheira, M., Coma, M., Fradinho, J., Carvalho, G., Oehmen, A., Reis, M.A.M. M.A.M., 2013. Determination of the extraction kinetics for the quantification of polyhydroxyalkanoate monomers in mixed microbial systems. Process Biochem. 48, 1626–1634. https://doi.org/http://dx.doi.org/10.1016/j.procbio.2013.07.023.

Laycock, B., Arcos-Hernandez, M.V., Langford, A., Buchanan, J., Halley, P.J., Werker, A., Lant, P.A., Pratt, S., 2014. Thermal properties and crystallization behavior of fractionated blocky and random polyhydroxyalkanoate copolymers from mixed microbial cultures. J. Appl. Polym. Sci. 131. https://doi.org/10.1002/app.40836.

Laycock, B., Arcos-Hernandez, M.V., Langford, A., Pratt, S., Werker, A., Halley, P.J., Lant, P.A., 2014. Crystallisation and fractionation of selected polyhydroxyalkanoates produced from mixed cultures. N. Biotechnol. 31, 345–356. https://doi.org/10.1016/j.nbt.2013.05.005.

Matos, M., Cruz, R.A.P., Cardoso, P., Silva, F., Freitas, E.B., Carvalho, G., Reis, M.A.M., 2021. Combined Strategies to Boost Polyhydroxyalkanoate Production from Fruit Waste in a Three-Stage Pilot Plant. ACS Sustain. Chem. Eng. 9, 8270–8279. https://doi.org/10.1021/acssuschemeng.1c02432.

Alcântara, Medeiros Garcia, J., Distante, F., Storti, G., Moscatelli, D., Morbidelli, M., Sponchioni, M.,, 2020. Current trends in the production of biodegradable bioplastics: The case of polyhydroxyalkanoates. Biotechnol. Adv.. https://doi.org/10.1016/j.biotechadv.2020.107582.

Moreira, F.S., Machado, R.G., Romão, B.B., Batista, F.R.X., Ferreira, J.S., Cardoso, V.L., 2017. Improvement of hydrogen production by biological route using repeated batch cycles. Process Biochem. 58, 60–68. https://doi.org/10.1016/j.procbio.2017.04.013.

Moretto, G., Russo, I., Bolzonella, D., Pavan, P., Majone, M., Valentino, F., 2020. An urban biorefinery for food waste and biological sludge conversion into polyhydroxyalkanoates and biogas. Water Res. 170. https://doi.org/10.1016/j.watres.2019.115371.

Morgan-Sagastume, F., Bengtsson, S., De Grazia, G., Alexandersson, T., Quadri, L., Johansson, P., Magnusson, P., Werker, A., 2020. Mixed-culture polyhydroxyalkanoate (PHA) production integrated into a food-industry effluent biological treatment: A pilot-scale evaluation. J. Environ. Chem. Eng. 8. https://doi.org/10.1016/j.jece.2020.104469.

Morgan-Sagastume, F., Hjort, M., Cirne, D., Gérardin, F., Lacroix, S., Gaval, G., Karabegovic, L., Alexandersson, T., Johansson, P., Karlsson, A., Bengtsson, S., Arcos-Hernández, M. V., Magnusson, P., Werker, A., 2015. Integrated production of polyhydroxyalkanoates (PHAs) with municipal wastewater and sludge treatment at pilot scale. Bioresour. Technol. 181, 78–89. https://doi.org/10.1016/j.biortech.2015.01.046.

Morgan-Sagastume, F., Pratt, S., Karlsson, A., Cirne, D., Lant, P., Werker, A., 2011. Production of volatile fatty acids by fermentation of waste activated sludge pre-treated in full-scale thermal hydrolysis plants. Bioresour. Technol. 102, 3089–3097. https://doi.org/10.1016/j.biortech.2010.10.054.

Oliveira, C.S.S., Silva, C.E., Carvalho, G., Reis, M.A., 2017. Strategies for efficiently selecting PHA producing mixed microbial cultures using complex feedstocks: Feast and famine regime and uncoupled carbon and nitrogen availabilities. N. Biotechnol. 37, 69–79. https://doi.org/10.1016/j.nbt.2016.10.008.

Oliveira, C.S.S., Silva, M.O.D., Silva, C.E., Carvalho, G., Reis, M.A.M., 2018. Assessment of protein-rich cheese whey waste stream as a nutrients source for low-cost mixed microbial PHA production. Appl. Sci. 8, 1817. https://doi.org/10.3390/app8101817.

Pereira, J.R., Araújo, D., Marques, A.C., Neves, L.A., Grandfils, C., Sevrin, C., Alves, V.D., Fortunato, E., Reis, M.A.M., Freitas, F., 2019. Demonstration of the adhesive properties of the medium-chain-length polyhydroxyalkanoate produced by Pseudomonas chlororaphis subsp. aurantiaca from glycerol. Int. J. Biol. Macromol. 122, 1144–1151. https://doi.org/10.1016/j.ijbiomac.2018.09.064.

Ramkumar, D.H.S., Bhattacharya, M., 1998. Steady shear and dynamic properties of biodegradable polyesters. Polym. Eng. Sci. 38, 1426–1435. https://doi.org/10.1002/pen.10313.

Sabapathy, P.C., Devaraj, S., Meixner, K., Anburajan, P., Kathirvel, P., Ravikumar, Y., Zabed, H.M., Qi, X., 2020. Recent developments in Polyhydroxyalkanoates (PHAs)

production – A review. Bioresour. Technol. 306. https://doi.org/10.1016/j.biortech.2020.123132.

Swiatkiewicz, J., Slezak, R., Krzystek, L., Ledakowicz, S., 2021. Production of Volatile Fatty Acids in a Semi-Continuous Dark Fermentation of Kitchen Waste: Impact of Organic Loading Rate and Hydraulic Retention Time. Energies. https://doi.org/10.3390/en14112993.

Valentino, F., Gottardo, M., Micolucci, F., Pavan, P., Bolzonella, D., Rossetti, S., Majone, M., 2018. Organic Fraction of Municipal Solid Waste Recovery by Conversion into Added-Value Polyhydroxyalkanoates and Biogas. ACS Sustain. Chem. Eng. 6, 16375–16385. https://doi.org/10.1021/acssuschemeng.8b03454.

Valentino, F., Karabegovic, L., Majone, M., Morgan-Sagastume, F., Werker, A., 2015. Polyhydroxyalkanoate (PHA) storage within a mixed-culture biomass with simultaneous growth as a function of accumulation substrate nitrogen and phosphorus levels. Water Res. 77, 49–63. https://doi.org/10.1016/j.watres.2015.03.016.

Valentino, F., Lorini, L., Gottardo, M., Pavan, P., Majone, M., 2020. Effect of the temperature in a mixed culture pilot scale aerobic process for food waste and sewage sludge conversion into polyhydroxyalkanoates. J. Biotechnol. 323, 54–61. https://doi.org/10.1016/j.jbiotec.2020.07.022.

Valentino, F., Moretto, G., Lorini, L., Bolzonella, D., Pavan, P., Majone, M., 2019. Pilot-Scale Polyhydroxyalkanoate Production from Combined Treatment of Organic Fraction of Municipal Solid Waste and Sewage Sludge. Ind. Eng. Chem. Res. 58, 12149–12158. https://doi.org/10.1021/acs.iecr.9b01831.

Wainaina, S., Awasthi, M.K., Horváth, I.S., Taherzadeh, M.J., 2020. Anaerobic digestion of food waste to volatile fatty acids and hydrogen at high organic loading rates in immersed membrane bioreactors. Renew. Energy 152, 1140–1148. https://doi.org/10.1016/j.renene.2020.01.138.